Redox Biology 1 (2013) 304–312

Contents lists available at SciVerse ScienceDirect

Redox Biology

journal homepage: www.elsevier.com/locate/redox

Research Paper

Sites of reactive oxygen species generation by mitochondria oxidizing different substrates ☆

Casey L. Quinlan [a,*], Irina V. Perevoshchikova [a], Martin Hey-Mogensen [a,b], Adam L. Orr [a], Martin D. Brand [a]

[a] The Buck Institute for Research on Aging, Novato, CA 94945, USA
[b] Department of Biomedical Sciences, Center for Healthy Aging, Copenhagen University, Denmark

ARTICLE INFO

Article history:
Received 22 March 2013
Received in revised form
4 April 2013
Accepted 5 April 2013

Keywords:
Superoxide
Hydrogen peroxide
Respiratory complexes
NADH
Ubiquinone
Cytochrome *b*

ABSTRACT

Mitochondrial radical production is important in redox signaling, aging and disease, but the relative contributions of different production sites are poorly understood. We analyzed the rates of superoxide/H_2O_2 production from different defined sites in rat skeletal muscle mitochondria oxidizing a variety of conventional substrates in the absence of added inhibitors: succinate; glycerol 3-phosphate; palmitoylcarnitine plus carnitine; or glutamate plus malate. In all cases, the sum of the estimated rates accounted fully for the measured overall rates. There were two striking results. First, the overall rates differed by an order of magnitude between substrates. Second, the relative contribution of each site was very different with different substrates. During succinate oxidation, most of the superoxide production was from the site of quinone reduction in complex I (site I_Q), with small contributions from the flavin site in complex I (site I_F) and the quinol oxidation site in complex III (site III_{Qo}). However, with glutamate plus malate as substrate, site I_Q made little or no contribution, and production was shared between site I_F, site III_{Qo} and 2-oxoglutarate dehydrogenase. With palmitoylcarnitine as substrate, the flavin site in complex II (site II_F) was a major contributor (together with sites I_F and III_{Qo}), and with glycerol 3-phosphate as substrate, five different sites all contributed, including glycerol 3-phosphate dehydrogenase. Thus, the relative and absolute contributions of specific sites to the production of reactive oxygen species in isolated mitochondria depend very strongly on the substrates being oxidized, and the same is likely true in cells and *in vivo*.

Introduction

An increasing number of hypotheses propose that production of mitochondrial reactive oxygen species (ROS) plays a crucial role in different areas of physiology and pathology [1–4]. Despite this, we know very little about which mitochondrial sites in the electron transport chain and associated metabolic enzymes are responsible for physiological or pathological ROS production under native conditions (*i.e.* in the absence of added inhibitors).

It is well established that isolated mitochondria can produce hydrogen peroxide (H_2O_2) *in vitro* [5,6]. Since the earliest observations by Chance and colleagues [7], this field has expanded considerably and many characteristics of mitochondrial superoxide/H_2O_2 production have been revealed. ROS are produced by the leak of electrons from donor redox centers to molecular oxygen. The mitochondrial electron transport chain (Fig. 1) consists of several complexes containing multiple redox centers that normally facilitate transfer of electrons to their final acceptor, molecular oxygen, which is reduced by four electrons to water at complex IV. Premature single electron reduction of molecular oxygen earlier in the chain forms the superoxide radical ($O_2^{\bullet-}$) and divalent reduction forms H_2O_2. Superoxide dismutase-2 in the matrix converts superoxide to H_2O_2, which can escape and be assayed in the surrounding medium. The general term 'ROS' can refer to several different species, but in this context we use it to refer only to superoxide or H_2O_2.

Using inhibitors to manipulate the redox states of particular sites and prevent superoxide generation from others, at least ten different sites of superoxide/H_2O_2 production in the electron transport chain and associated enzymes (Krebs cycle, β-oxidation etc.) have been identified in mammalian mitochondria (Fig. 1).

Abbreviations: I_F, flavin site of complex I; I_Q, quinone-binding site of complex I; II_F, flavin site of complex II; III_{Qo}, quinol oxidation site of complex III; CDNB, 1-chloro-2,4-dinitrobenzene; E_h, redox potential; ETF, electron transferring flavoprotein; ETF:QOR, ETF:ubiquinone oxidoreductase; mGPDH, mitochondrial glycerol 3-phosphate dehydrogenase; OGDH, 2-oxoglutarate dehydrogenase; PDH, pyruvate dehydrogenase; Q, ubiquinone; QH_2, ubiquinol; ROS, reactive oxygen species.

* Correspondence to: The Buck Institute for Research on Aging, 8001 Redwood Blvd., Novato, CA 94945, USA. Tel.: +1 415 493 3676.
E-mail address: cquinlan@buckinstitute.org (C.L. Quinlan).

2213-2317/$ - see front matter © 2013 The Authors. Published by Elsevier B.V. All rights reserved.
http://dx.doi.org/10.1016/j.redox.2013.04.005

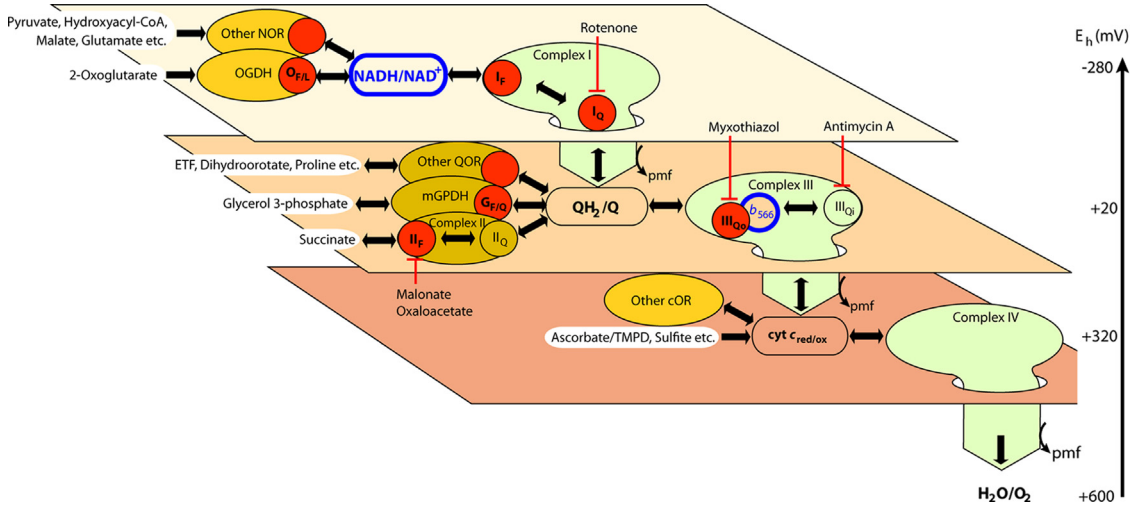

Fig. 1. Isopotential groups, electron flow, and endogenous reporters of superoxide/H_2O_2 production at different sites in mitochondria. The three planes represent different isopotential groups of redox centers, each operating at about the same redox potential (E_h): NADH/NAD$^+$ at E_h~−280 mV, QH_2/Q at E_h~+20 mV, and cytochrome *c* at E_h~+320 mV [31]. The normal flow of electrons from substrate dehydrogenases through NADH to oxygen is indicated by the large green arrows dropping down through the isopotential planes. The enzymes that feed electrons into each isopotential group are represented as ovals, and relevant inhibitors are drawn with blunted arrows. Electrons from NAD-linked substrates enter the NADH/NAD$^+$ pool at E_h~−280 mV through appropriate NAD oxidoreductases (NOR) including 2-oxoglutarate dehydrogenase (OGDH) and malate dehydrogenase (MDH) and flow into complex I (site I_F). They then drop down via site I_Q to QH_2/Q at E_h~+20 mV in the next isopotential pool, providing the energy to pump protons and generate protonmotive force (pmf). Q oxidoreductases (QOR) including complex II and mitochondrial glycerol 3-phosphate dehydrogenase (mGPDH) can also pass electrons into the Q pool. Electrons flow from QH_2 through complex III to cytochrome *c* at E_h~+320 mV in the next isopotential pool, again pumping protons and generating pmf. Ascorbate plus *N*,*N*,*N*′,*N*′-tetramethyl-phenylenediamine (TMPD) and cytochrome *c* oxidoreductases including sulfite oxidase can also pass electrons to cytochrome *c*. Finally, electrons flow through complex IV to oxygen at E_h~+600 mV, generating pmf. The redox state of NADH (outlined in blue), measured as NAD(P)H using autofluorescence, reports the redox state of the first isopotential group. The redox state of cytochrome b_{566} (outlined in blue), measured using absorbance spectroscopy, reports the redox state of the second isopotential group [21]. Red dots are sites of superoxide/H_2O_2 production. Named sites are the flavin/lipoate of 2-oxoglutarate dehydrogenase ($O_{F/L}$), the complex I flavin and Q-binding sites (I_F and I_Q, respectively), the flavin site of complex II (II_F), the flavin/quinone site of mGPDH ($G_{F/Q}$), and the outer quinol-binding site of complex III (III_{Qo}). Other sites, both known and unknown, are indicated by unlabeled red dots. These include less well-described sites such as pyruvate dehydrogenase, the ETF/ETF:QOR system, proline dehydrogenase, and dihydroorotate dehydrogenase.

Each of these sites has been at least partially characterized. The sites that are often invoked as the most important mitochondrial superoxide producers are in respiratory complexes I and III [5,6]. In complex I there are two sites: the flavin in the NADH-oxidizing site (site I_F) and the ubiquinone-reducing site (site I_Q) [8]. In complex III, the superoxide is thought to arise from the quinol oxidizing site (site III_{Qo}) [9–11]. However, other sites of superoxide/H_2O_2 production have also been defined, including 2-oxoglutarate dehydrogenase (OGDH) [12,13]; pyruvate dehydrogenase (PDH) [14]; complex II (site II_F) [15]; and glycerol 3-phosphate dehydrogenase (mGPDH) [16]. In addition, there are suggestions that other less well-described sites may also be involved in H_2O_2 production: the electron transferring flavoprotein/ETF:Q oxidoreductase (ETF/ETF:QOR) system of fatty acid β-oxidation [17,18]; proline dehydrogenase [19]; and dihydroorotate dehydrogenase [16,20].

Despite our understanding of the superoxide/H_2O_2-producing capacities of mitochondrial enzymes *in vitro*, we know very little about the native ROS-producing behavior of mitochondria *in vitro* or *in situ*. This is because the standard way to implicate a specific ROS-producing site in a particular phenotype is to inhibit or genetically modify the site, and observe the change in ROS signal or in the downstream phenotype. However, this approach is fundamentally flawed, because blocking a site of electron transport will invariably interrupt normal electron flow and alter the redox states of other sites in the electron flow pathway, which can dramatically alter their rates of ROS production, leading to unreliable or incorrect conclusions. This raises the question: how can the individual contributions from a complex suite of superoxide/H_2O_2-producing sites be assessed within intact mitochondria under native conditions? To address this question, we developed a novel method of estimating the rates of superoxide generation from two specific sites (I_F and III_{Qo}) by determining the dependence of superoxide production from each site (defined using inhibitors) on the redox state of its electron donor (reported by the redox states of NAD(P)H and cytochrome b_{566}, respectively), then measuring the redox state of the reporter under native conditions in the absence of added inhibitors to predict the contribution of the reported site to overall H_2O_2 production [21].

In the present study, we extend this approach of using endogenous reporters under native conditions to encompass many more superoxide/H_2O_2-producing sites and a greater variety of substrates. We determine the contributions of each site to overall H_2O_2 production by isolated skeletal muscle mitochondria oxidizing four different substrate combinations in the absence of inhibitors: (a) succinate, (b) glycerol 3-phosphate, (c) palmitoylcarnitine plus carnitine, and (d) glutamate plus malate. The results show that the absolute and relative contribution of each site differs greatly with different substrates.

Materials and methods

Animals, mitochondrial preparation, and reagents

Female Wister rats (Harlan Laboratories), age 5–8 weeks, were fed chow *ad libitum* and given free access to water. Mitochondria from hind limb skeletal muscle were isolated at 4 °C in Chappell–Perry buffer (CP1; 100 mM KCl, 50 mM Tris, 2 mM EGTA, pH 7.1 at 25 °C) by standard procedures [22]. The animal protocol was approved by the Buck Institute Animal Care and Use Committee, in accordance with IACUC standards. All reagents were from Sigma except Amplex UltraRed, which was from Invitrogen.

Superoxide/H_2O_2 production

Rates of superoxide/H_2O_2 production were measured collectively as rates of H_2O_2 production, as two superoxide molecules are dismutated by endogenous or exogenous superoxide dismutase to yield one H_2O_2. H_2O_2 was detected using the horseradish peroxidase

and Amplex UltraRed detection system [22]. Mitochondria (0.3 mg protein ml^{-1}) were suspended under non-phosphorylating conditions in medium at 37 °C containing 120 mM KCl, 5 mM Hepes, 5 mM K_2HPO_4, 2.5 mM $MgCl_2$, 1 mM EGTA, and 0.3% (w/v) bovine serum albumin (pH 7.0 at 37 °C), together with 5 U ml^{-1} horseradish peroxidase, 25 U ml^{-1} superoxide dismutase, 50 μM Amplex UltraRed and, except for experiments with palmitoylcarnitine, 1 μg ml^{-1} oligomycin. Reactions were monitored fluorometrically in a Shimadzu RF5301-PC or Varian Cary Eclipse spectrofluorometer ($\lambda_{excitation}$= 560 nm, $\lambda_{emission}$=590 nm) with constant stirring, and calibrated with known amounts of H_2O_2 [22].

To correct for losses of H_2O_2 caused by peroxidase activity in the matrix and give a better estimate of superoxide/H_2O_2 production rates, all H_2O_2 production rates were mathematically corrected to the rates that would have been observed in these mitochondria after pre-treatment with 1-chloro-2,4-dinitrobenzene (CDNB) to deplete glutathione and decrease glutathione peroxidase and peroxiredoxin activity, as described in Refs. [21,23], using an empirical equation

$$v_{CDNB} = v_{control} + (100 \times v_{control})/(72.6 + v_{control}) \quad (1)$$

(rates in pmol H_2O_2 min^{-1} mg $protein^{-1}$).

NAD(P)H redox state

Experiments were performed using 0.3 mg mitochondrial protein ml^{-1} at 37 °C in parallel with measurements of H_2O_2 production and cytochrome b_{566} redox state in the same medium with the same additions. The reduction state of endogenous NAD(P)H was determined by autofluorescence (most of the autofluorescence signal is from NADH bound in the matrix, and NADPH hardly changes in our experiments, but for full disclosure we use "NAD(P)H") [21,23] using a Shimadzu RF5301-PC or Varian Cary Eclipse spectrofluorometer at $\lambda_{excitation}$=365 nm, $\lambda_{emission}$=450 nm. NAD(P)H was assumed to be 0% reduced after 5 min without added substrate and 100% reduced with 5 mM malate plus 5 mM glutamate and 4 μM rotenone. Intermediate values were determined as % reduced NAD(P)H relative to the 0% and 100% values.

Cytochrome b_{566} redox state

Experiments were performed at 1.5 mg mitochondrial protein ml^{-1} in parallel with measurements of H_2O_2 production and NAD(P)H redox state in the same medium. The reduction state of endogenous cytochrome b_{566} was measured with constant stirring at 37 °C in an Olis DW-2 dual wavelength spectrophotometer as the absorbance difference at 566–575 nm [11,21]. Cytochrome b_{566} was assumed to be 0% reduced after 5 min without added substrate and 100% reduced with saturating substrates plus antimycin A. Intermediate values were determined as % reduced b_{566} relative to the 0% and 100% values.

Definition of sites and calibration of endogenous reporters

Site I_F was defined as the site producing superoxide (measured as H_2O_2) in the presence of malate to reduce NAD to NADH, and rotenone to inhibit reoxidation of complex I by the Q-pool. Any H_2O_2 arising from reverse flow from the NADH pool into NAD oxidoreductases such as OGDH or PDH will appear in the analysis as a component of site I_F (Fig. 2a). To decrease the contributions of forward electron flow at OGDH and PDH to H_2O_2 production

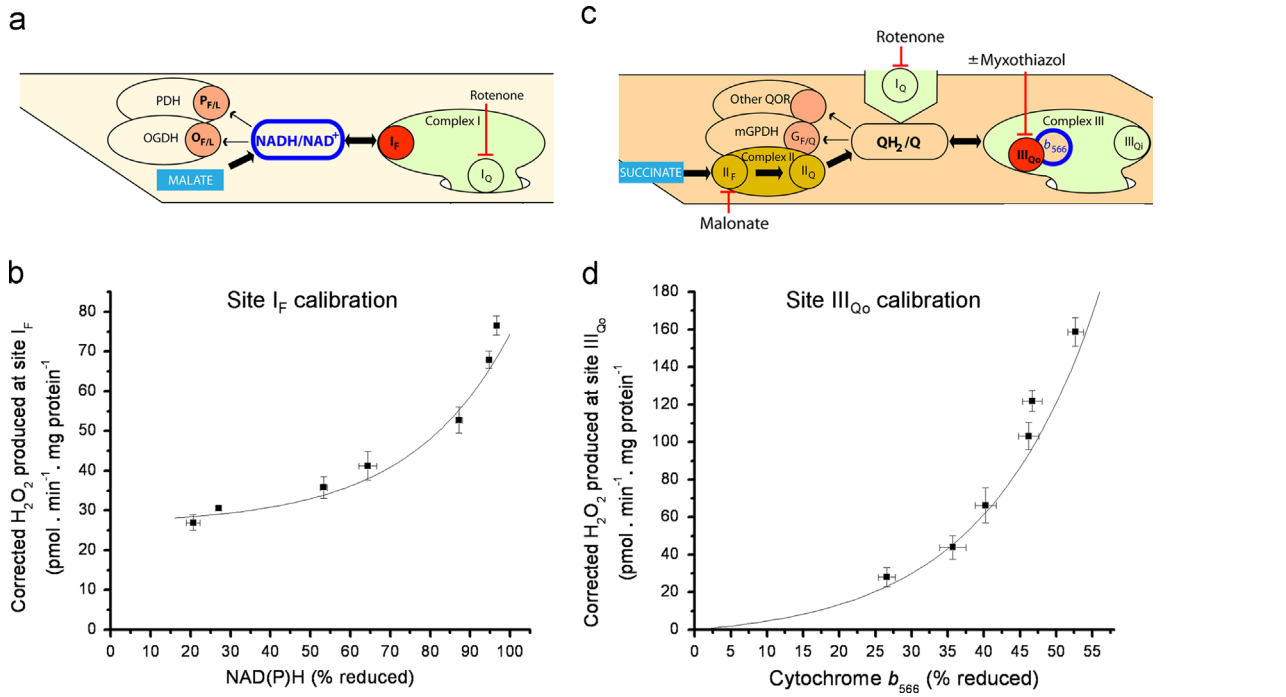

Fig. 2. Calibration of endogenous reporters in isolated rat skeletal muscle mitochondria. (a) Definition of site I_F (red dot) using malate as substrate in the presence of rotenone to inhibit site I_Q and cause reduction of upstream sites and oxidation of all downstream sites. The definition includes any small contribution from backflow of electrons from NADH into other sites, e.g. OGDH and PDH, shown in pink. $P_{F/L}$ denotes the flavin/lipoate of pyruvate dehydrogenase. (b) Dependence of superoxide production (measured as extramitochondrial appearance of H_2O_2) from site I_F on the redox state of NAD(P)H (measured by autofluorescence). Malate was titrated from 20 μM −5 mM in the presence of 4 μM rotenone, 1.5 mM aspartate and 2.5 mM ATP. (c) Definition of site III_{Qo} (red dot) using succinate as substrate, rotenone to inhibit site I_Q, and sufficient succinate+malonate (5 mM) to suppress site II_F. The rate of superoxide/H_2O_2 production from site III_{Qo} was defined as the rate that was inhibited by 2 μM myxothiazol (after correction for changes at site I_F using the calibration curve in (b)). The definition includes any small contribution from backflow of electrons from QH_2 into other sites, e.g. mGPDH or other Q-oxidoreductases, shown in pink. (d) Dependence of myxothiazol-sensitive superoxide production from site III_{Qo} on the redox state of cytochrome b_{566} (measured by the absorbance spectroscopy). Electron input was titrated by adding different ratios of succinate:malonate (sum=5 mM) in the presence of 4 μM rotenone. Data are means ± SEM (n≥4) recalculated from [21] using the new calibration in (b). For curve-fitting see Materials and methods.

assigned to site I_F, we added 1.5 mM aspartate to remove endogenous 2-oxoglutarate by transamination and 2.5 mM ATP to decrease carbon flows at various points in the Krebs cycle, particularly succinate thiokinase. This change to our previous protocol [18,21] strongly decreased our earlier estimates of the rates from site I_F. The rate of superoxide/H_2O_2 production from site I_F defined by inhibitors in this way was measured as a function of the redox state of NAD(P)H at different malate concentrations between 0.02 mM and 5 mM (Fig. 2b). The data were arbitrarily fitted by non-linear regression to a single exponential, to give the parameter values in the following equation:

$$v_{H_2O_2(\%NAD(P)H)} = 0.88 \times e^{(0.04(\%NAD(P)H))} + 26.5 \quad (2)$$

where $v_{H_2O_2}$ is the rate of H_2O_2 production. This equation was used to predict the rate of superoxide/H_2O_2 production from site I_F at any observed NAD(P)H redox state in the absence of inhibitors in subsequent experiments.

Superoxide production by site III_{Qo} was measured as H_2O_2 production in the presence of succinate to reduce the Q pool, malonate to keep total succinate plus malonate at 5 mM and inhibit superoxide/H_2O_2 formation from site II_F without fully inhibiting succinate oxidation [15], and rotenone to inhibit superoxide formation from site I_Q (Fig. 2c). Site III_{Qo} was defined as the component of the observed H_2O_2 production under these conditions that was sensitive to myxothiazol (a specific inhibitor of site III_{Qo}) after correction for the small difference in rates from site I_F before and after myxothiazol addition (calculated from parallel measurements of NAD(P)H and application of the calibration curve in Fig. 2b). The rate of superoxide/H_2O_2 production from site III_{Qo} defined by inhibitors in this way was measured as a function of the redox state of cytochrome b_{566} at different succinate: malonate ratios ranging from 75% to 100% succinate at 5% increments (total dicarboxylate concentration 5 mM) (Fig. 2d). The data were arbitrarily fitted in the same way as for site I_F to give the parameter values using the following equation:

$$v_{H_2O_2(\%b_{566})} = 5.22 \times e^{(0.064(\%b_{566}))} - 5.22 \quad (3)$$

This equation was used to predict the rate of superoxide/H_2O_2 production from site III_{Qo} at any observed cytochrome b_{566} redox state in the absence of inhibitors in subsequent experiments.

See Ref. [21] for more extensive discussion and descriptions.

Statistics

When using the calibration curves in Fig. 2 to calculate rates of H_2O_2 production at a given reduction state of the reporter, the error in the measurements during calibration was taken into account. This error was calculated by standard methods of error propagation through all the steps, as detailed in [21].

The significance of differences between reported and experimentally measured rates of H_2O_2 production in each experimental condition was tested using Welch's *t*-test. Because error propagation was used to capture uncertainty in the calibration curves, individual data-points could not be used for statistical analysis. Instead we used the traits describing the population of data (mean, SEM based on error propagation and number of observations) to calculate if differences were significant ($p < 0.05$).

Results and discussion

The aim of the present study was to determine the contributions of different sites of superoxide/H_2O_2 production to the total observed H_2O_2 generation by mitochondria during oxidation of different substrates in the absence of inhibitors. Electrons leak from the respiratory chain to generate superoxide or H_2O_2 at two different redox potentials (E_h): at the isopotential group of redox carriers around the NADH/NAD^+ pool at E_h~−280 mV and at the isopotential group of redox carriers around the QH_2/Q pool at E_h~+20 mV (Fig. 1). At each isopotential group, an important determinant of the rate of superoxide or H_2O_2 production is the redox state: a more reduced carrier generally leaks electrons to oxygen at a faster rate. We exploited this relationship to create assays of the rate of superoxide/H_2O_2 production from different sites, either by defining the site precisely with inhibitors and determining its dependence on the redox state of the appropriate pool as described in Materials and methods (Fig. 2), or by inhibiting the site and determining the change in superoxide/H_2O_2 production after correction for secondary changes in the redox states of the two pools. Specifically, to predict rates from each site with different respiratory substrates in the absence of inhibitors, we measured the redox states of the endogenous reporters NAD(P)H and cytochrome b_{566} as proxies of the redox states of the two isopotential groups, and determined the rates of superoxide/H_2O_2 production from sites I_F and III_{Qo}, respectively, using the calibration curves in Fig. 2. Assessing the contribution of other sites was a little more complicated, so we first provide an example of how the endogenous reporter calibration curves and the careful use of inhibitors can be used to quantify the sites of H_2O_2 production during oxidation of the substrate succinate.

Sites of superoxide/H_2O_2 production during oxidation of succinate: a worked example

When succinate is oxidized in the absence of rotenone and other electron transport chain inhibitors, electrons flow through complex II into the Q pool. Next, there are two options (Fig. 3a). The electrons can flow forward to complex III and thermodynamically downhill to more oxidized isopotential groups at cytochrome *c* and H_2O/O_2, pumping protons at complexes III and IV and generating protonmotive force. Alternatively, they can flow in reverse to complex I, driven thermodynamically uphill to the more negative isopotential group by reversal of the proton pumps in complex I driven by the protonmotive force generated by proton pumping at complexes III and IV. In the process, a number of possible sites of superoxide/H_2O_2 production may be engaged, particularly sites II_F, III_{Qo}, I_Q and I_F (Fig. 3a). However, it is generally agreed that the primary mechanism of H_2O_2 production during succinate oxidation is reverse electron transport into complex I, because this H_2O_2 production is very sensitive to rotenone, the classic Q-site inhibitor of complex I [24,25]. What is not usually discussed is that when an inhibitor such as rotenone is added there are subsequent shifts in electron distribution that invariably change the rates of superoxide/H_2O_2 production by sites both upstream and downstream of the inhibition site [21]. Therefore, the decrease in rate observed after the addition of an inhibitor is not an accurate indication of the rate from its target site before inhibition. The endogenous reporter method described here circumvents this problem: by monitoring the changes in the NADH isopotential group (through NAD(P)H) and the Q isopotential group (through cytochrome b_{566}), the changes in electron distribution after inhibitors are added can be quantified and corrected for.

In this worked example, we quantified the sites of H_2O_2 production during succinate oxidation by measuring the redox states of the endogenous reporters, and the changes in these redox states after addition of rotenone. From this information, we could predict the contribution of each site to the total H_2O_2 production observed during succinate oxidation. To begin, we measured the rate of H_2O_2 production during succinate oxidation in the absence of rotenone (891 pmol H_2O_2 min^{-1} mg $protein^{-1}$) (Fig. 4a). In parallel, in different cuvettes, we measured the reduction states of the reporters. We observed that NAD(P)H was 89% reduced and cytochrome b_{566} was 46% reduced (Fig. 4b, Table 1). From

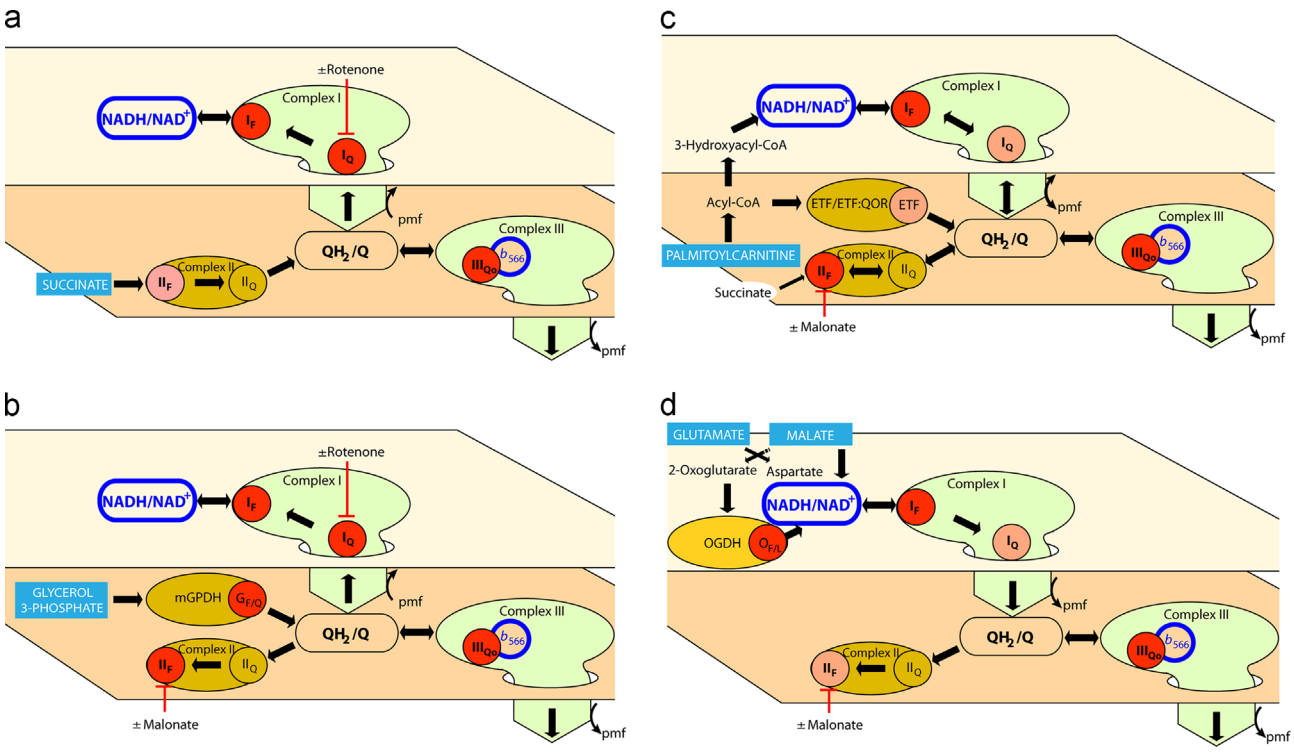

Fig. 3. Electron flows and sites of superoxide/H_2O_2 production during oxidation of different substrates by rat skeletal muscle mitochondria. Electron flows and postulated (red and pink dots) and observed (red dots) sites of superoxide/H_2O_2 production during oxidation of (a) succinate, (b) glycerol 3-phosphate, (c) palmitoylcarnitine plus carnitine and (d) glutamate plus malate.

this information, we could predict using the equations describing the calibration curves in Fig. 2 that site I_F was producing 59 pmol H_2O_2 min^{-1} mg $protein^{-1}$ (7% of the total), and site III_{Qo} was producing 91 pmol H_2O_2 min^{-1} mg $protein^{-1}$ (10%) (Fig. 4c, Table 1), with the remaining 741 pmol H_2O_2 min^{-1} mg $protein^{-1}$ coming from other sites.

To identify and quantify these other sites, we added rotenone to inhibit site I_Q, and measured the changes in H_2O_2 production and the changes in the reduction state of the reporters (Figs. 4a and b, Table 1). After rotenone addition, the overall rate of H_2O_2 production dropped to 131 pmol H_2O_2 min^{-1} mg $protein^{-1}$, NAD(P)H became significantly more oxidized and cytochrome b_{566} appeared to become slightly more reduced (Fig. 4 a and b, Table 1). Again, using the calibration curves in Fig. 2 we determined that site I_F now appeared to produce slightly less superoxide/H_2O_2 (49 pmol H_2O_2 min^{-1} mg $protein^{-1}$) and site III_{Qo} appeared to produce more (124 pmol H_2O_2 min^{-1} mg $protein^{-1}$) than before the addition of rotenone (Fig. 4c, Table 1). When rotenone was added, not only was reverse electron flow abolished, leading to partial oxidation of NAD(P)H as the electron supply from succinate through complex I failed, but there appeared to be a small increase in the reduction level of cytochrome b_{566} as all flow was diverted through complex III. The total change in superoxide/H_2O_2 production at site I_F was calculated by subtracting the rate before rotenone addition (59 pmol H_2O_2 min^{-1} mg $protein^{-1}$) from the rate after rotenone addition (49 pmol H_2O_2 min^{-1} mg $protein^{-1}$) to give a final change in rate from site I_F of −10 pmol H_2O_2 min^{-1} mg $protein^{-1}$. The equivalent calculation performed for site III_{Qo} gave a total change of +33 pmol H_2O_2 min^{-1} mg $protein^{-1}$. The rotenone-sensitive rate (759 pmol H_2O_2 min^{-1} mg $protein^{-1}$) was then corrected for the changes in superoxide/H_2O_2 production from sites I_F and III_{Qo} to give a final adjusted rate of 736 pmol H_2O_2 min^{-1} mg $protein^{-1}$, all assigned to site I_Q (it was not from site I_F, as has been suggested [26], because site I_F superoxide production was fully corrected for using NAD(P)H as the endogenous reporter). This painted a final picture (Fig. 4d) showing that during succinate oxidation, site I_Q contributed 83% of the observed rate of H_2O_2 production while site I_F accounted for 7% and site III_{Qo} accounted for 10%. Since there was no unaccounted-for rate of H_2O_2 production, either before (891 pmol H_2O_2 min^{-1} mg $protein^{-1}$ observed *versus* 886 pmol H_2O_2 min^{-1} mg $protein^{-1}$ assigned, N.S.) or after addition of rotenone (131 pmol H_2O_2 min^{-1} mg $protein^{-1}$ observed *versus* 171 pmol H_2O_2 min^{-1} mg $protein^{-1}$ assigned, N.S.), no other site made a substantial contribution to the total observed rate. The reason site II_F did not contribute is that the conventional succinate concentration used (5 mM) was sufficiently high to effectively abolish production of superoxide/H_2O_2 by site II_F [15].

There are no surprises in these conclusions (although they are more accurate than simply assigning the rotenone-sensitive signal to complex I): site I_Q is the dominant superoxide/H_2O_2 producer when succinate is oxidized in the absence of rotenone. However, this example illustrates clearly that during oxidation of a single substrate, superoxide/H_2O_2 are produced from multiple sites (Fig. 4d). It also clearly illustrates that site-specific inhibitors not only affect superoxide/H_2O_2 production at the site that they inhibit, but also (through changes in electron distribution) change superoxide/H_2O_2 production at other sites.

The contributions of specific sites to superoxide/H_2O_2 production during oxidation of different substrates

The approach described above as a worked example using succinate as substrate was used to define the contributions of specific sites to superoxide/H_2O_2 production during oxidation of three additional important conventional substrates: glycerol 3-phosphate, palmitoylcarnitine plus carnitine, and glutamate plus malate. In each condition, the reduction state of the reporters was measured in parallel with H_2O_2 production. The changes in reduction state of the reporters after addition of inhibitors of complex I or complex II were measured and used to correct for consequent changes in electron distribution and superoxide/H_2O_2 production at other sites. Table 1 details the observed redox states

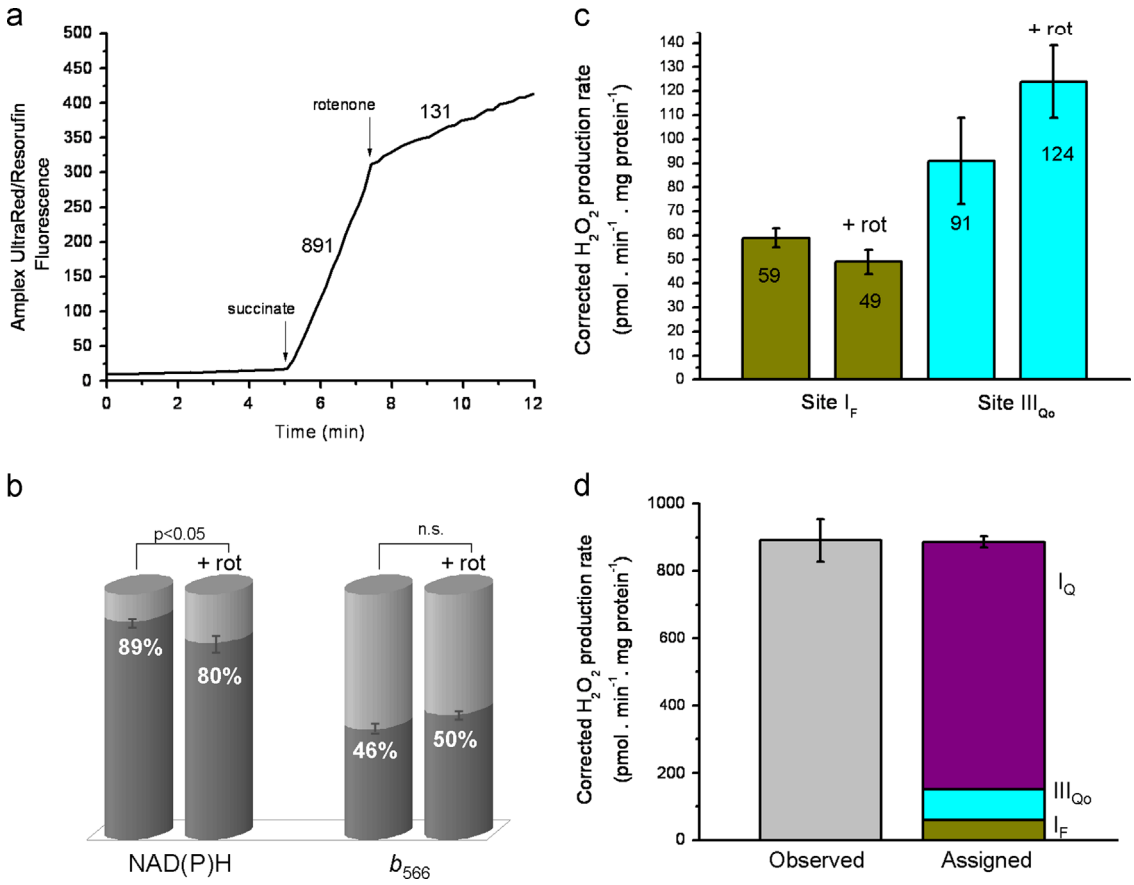

Fig. 4. Sites of superoxide/H_2O_2 production during succinate oxidation: a worked example. (a) Representative trace of Amplex UltraRed/resorufin fluorescence during oxidation of 5 mM succinate by rat skeletal muscle mitochondria before and after addition of 4 μM rotenone. Numbers by the traces represent average calibrated rates in pmol H_2O_2 min^{-1} mg protein^{-1}. (b) Reduction states of the endogenous reporters NAD(P)H and cytochrome b_{566} before and after rotenone addition. The difference in reduction state before and after rotenone was significant for NAD(P)H ($p=0.01$), but not for cytochrome b_{566} ($p=0.11$) by Student's t-test. (c) Rates of superoxide/H_2O_2 production from sites I_F and III_{Qo} before and after rotenone addition, predicted from (b) using the calibration curves in Fig. 2. Results are means ± SEM ($n=4$). To account for error in both the measurements and the calibration curves, a Welch's t-test was used. The difference in rates before and after rotenone did not fall within the 95% confidence interval ($p=0.09$ for site I_F and 0.15 for III_{Qo}). (d) Observed total rate of H_2O_2 production during succinate oxidation (before addition of rotenone) and assigned rates of superoxide/H_2O_2 production from sites I_F, III_{Qo} and I_Q during succinate oxidation. Results are means ± SEM ($n=4$); the error bars on the sum column show the combined propagated errors in the total sum value. There was no significant difference between the observed rate and the sum of the assigned rates (Welch's t-test; $p<0.05$).

of the reporters with each substrate before and after addition of the inhibitors rotenone or malonate.

Fig. 5 shows the central result of the present paper: the contributions of each of the individual sites of superoxide/H_2O_2 production to overall H_2O_2 generation by isolated skeletal muscle mitochondria with each of the four substrate combinations under native conditions in the absence of added inhibitors. The first striking result is that the overall rates of H_2O_2 generation were very different with different substrates, as previously observed by [27] and others [28–30]. The second, crucial, observation is that the relative contribution of each site was very different with different substrates. Thus, the relative and absolute contributions of specific sites to the production of reactive oxygen species in isolated mitochondria depend very strongly on the substrates being oxidized.

To determine the contributions of individual sites to overall H_2O_2 generation with each substrate, the rates of H_2O_2 production at site I_F and III_{Qo} were first estimated from the redox states of NAD(P)H and cytochrome b_{566} using the calibration curves in Fig. 2. With succinate and glycerol 3-phosphate, the contribution of site I_Q was then estimated from the decrease in the rate of H_2O_2 production after addition of rotenone followed by correction for changes in the rate from site I_F (calculated from the redox state of NAD(P)H before and after rotenone addition using the calibration curve in Fig. 2a) and from site III_{Qo} (calculated from the redox state of cytochrome b_{566} before and after rotenone addition using the calibration curve in Fig. 2c). With glycerol 3-phosphate, palmitoylcarnitine plus carnitine, and glutamate plus malate, the contribution of site II_F was estimated from the decrease in rate of H_2O_2 production after addition of malonate followed by correction for changes in the rate from site I_F (calculated from the redox state of NAD(P)H before and after malonate addition) and from site III_{Qo} (calculated from the redox state of cytochrome b_{566} before and after malonate addition). The contributions of mGPDH (with glycerol 3-phosphate as substrate) and OGDH (with glutamate plus malate as substrate) were estimated as the difference between the sum of the rates estimated for the other sites and the observed total rate.

Sites of superoxide/H_2O_2 production during oxidation of glycerol 3-phosphate

Glycerol 3-phosphate oxidation by mGPDH results directly in Q pool reduction (Fig. 3b). From the Q pool, electrons may flow both forward (to complex III and beyond, generating protonmotive force) and in reverse (to complex I and complex II). In the process, a number of possible sites of superoxide/H_2O_2 production may be engaged, particularly mGPDH and sites II_F, III_{Qo}, I_Q and I_F (Fig. 3b). Protonmotive force is required for reverse electron flow to complex I [25], but not for reversal into complex II [16]. Complex II has

been shown to generate superoxide in both the forward and reverse reactions [15].

With glycerol 3-phosphate as substrate, the total observed rate of H_2O_2 production was 622 pmol H_2O_2 min^{-1} mg $protein^{-1}$. Sites I_F (6%) and III_{Qo} (4%) made only modest contributions to this total rate (Fig. 5). The contributions of sites I_Q (33%) and II_F (26%) (after correction for changes in sites I_F and III_{Qo} following the addition of inhibitors) were more substantial. The absolute rates from sites I_F, III_{Qo} and I_Q were lower with glycerol 3-phosphate than with succinate, because the two isopotential pools were less reduced (Table 1), presumably because succinate was a better substrate than glycerol 3-phosphate in this experiment, which had sub-optimal glycerol 3-phosphate and calcium concentrations. After these assignments, 192 pmol H_2O_2 min^{-1} mg $protein^{-1}$ (31% of the total) remained unaccounted for. mGPDH itself is known to generate ROS (predominantly superoxide), which are released to both the matrix and the intermembrane space [16]. In this case, we assume that the remaining observed rates of H_2O_2 production must have arisen from mGPDH, since all other known sites were already accounted for, and we assign this site by difference (31%). It is unlikely that any of the unassigned H_2O_2 generation in this condition was from uncharacterized sites, since such sites would have to be engaged during oxidation of glycerol 3-phosphate but not during oxidation of succinate (where there was no unassigned H_2O_2 production, Fig. 5), despite the less extensive reduction of the two isopotential groups with glycerol 3-phosphate as substrate (Table 1).

Sites of superoxide/H_2O_2 production during oxidation of palmitoylcarnitine plus carnitine

Carnitine enhances oxidation of palmitoylcarnitine by removing inhibitory acetyl-CoA in the form of acetylcarnitine and by promoting entry of palmitoylcarnitine into the mitochondrial matrix [18]. When palmitoylcarnitine is metabolized by the β-oxidation pathway, electrons enter the respiratory chain at two sites: from acyl-CoA dehydrogenase through the electron transferring flavoprotein (ETF) and ETF:ubiquinone oxidoreductase (ETF:QOR) to the Q-pool, and from 3-hydroxyacyl-CoA dehydrogenase to NADH (Fig. 3c). Oxidation of the end product, acetyl-CoA, in the citric acid cycle leads to further electron input through the NAD-linked dehydrogenases and through complex II during oxidation of succinate. Electron entry by more than one route suggests that

Table 1
Reduction levels of reporters and corresponding calculated rates of H_2O_2 production from site I_F and site III_{Qo} in the presence of different substrates and inhibitors. With each substrate, the redox states of NAD(P)H and cytochrome b_{566} were measured in parallel with the measurements of overall rates of H_2O_2 production reported in Fig. 5. Eqs. (2) and (3) describing the calibration curves in Fig. 2 were used to calculate the rates of superoxide/H_2O_2 production from site I_F and site III_{Qo} from these redox measurements. Concentrations of substrates and inhibitors are given in Fig. 5. All rates are in pmol H_2O_2 min^{-1} mg $protein^{-1}$. Data are means ± SEM ($n \geq 4$). Error values on the calculated rates of H_2O_2 production represent the propagated error as described in Materials and methods and Ref. [21].

Substrates and inhibitors	Redox state of site I_F reporter and calculated rate of superoxide/H_2O_2 production by site I_F		Redox state of site III_{Qo} reporter and calculated rate of superoxide/H_2O_2 production by site III_{Qo}	
	Reduced NAD(P)H (%)	Reported rate of H_2O_2 production	Reduced cytochrome b_{566} (%)	Reported rate of H_2O_2 production
Succinate	89 ± 1	59 ± 4	46 ± 2	91 ± 18
Succinate+rotenone	80 ± 2	49 ± 4	50 ± 1	124 ± 15
Glycerol 3-phosphate	59 ± 3	34 ± 6	29 ± 2	27 ± 7
Glycerol 3-phosphate+malonate	59 ± 3	34 ± 6	29 ± 2	27 ± 7
Glycerol 3-phosphate+malonate+rotenone	39 ± 2	31 ± 5	31 ± 3	33 ± 9
Palmitoylcarnitine+carnitine	80 ± 1	49 ± 4	42 ± 3	72 ± 18
Palmitoylcarnitine+carnitine+malonate	79 ± 1	48 ± 4	44 ± 2	80 ± 17
Glutamate+malate	85 ± 7	54 ± 9	38 ± 5	54 ± 18

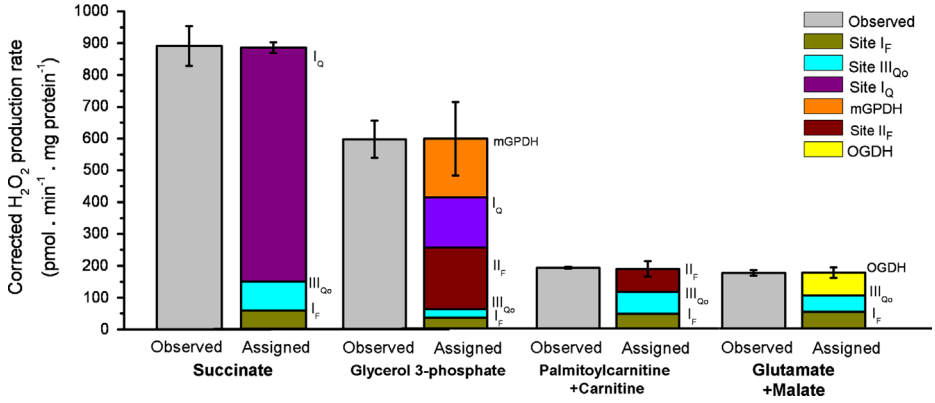

Fig. 5. Native rates of superoxide/H_2O_2 production by mitochondria oxidizing different substrates. Observed total rate of H_2O_2 production (gray bars) and sum of assigned rates of superoxide/H_2O_2 production from different sites (colored stacked bars) in the presence of different substrates as indicated: 5 mM succinate; 27 mM disodium *rac*-α/β-glycerol phosphate (25% active optical isomer *sn*-glycerol 3-phosphate); 15 μM palmitoyl-L-carnitine plus 2 mM L-carnitine; and 5 mM L-glutamate plus 5 mM L-malate. With each substrate, the reduction states of NAD(P)H and cytochrome b_{566} were measured in parallel with H_2O_2 production and the calibration curves in Fig. 2 were used to predict the rates of production from sites I_F and III_{Qo}. With succinate, 4 μM rotenone was subsequently added to allow calculation of the rate from site I_Q as described in the text (data from Fig. 4d). With glycerol 3-phosphate, 1 mM malonate and 4 μM rotenone were subsequently added to allow calculation of the rates from sites II_F and I_Q, respectively. The rate assigned to mGPDH was calculated by difference. With palmitoylcarnitine plus carnitine, 1 mM malonate was subsequently added to allow calculation of the rate from site II_F (data recalculated from [18]). With glutamate plus malate, the rate assigned to OGDH was calculated by difference (data recalculated from [21]). Results are means ± SEM (n=4–6); the error bars on the sum columns show the combined propagated errors in the total sum value. There was no significant difference between observed and assigned rates with succinate or with palmitoylcarnitine plus carnitine (Welch's t-test; $p < 0.05$).

fatty acid oxidation may generate superoxide/H_2O_2 from several different sites, particularly ETF/ETF:QOR and sites III_{Qo}, I_Q and I_F (Fig. 3c). Site II_F may also contribute by reverse flow from the Q pool, or by forward flow from succinate. Importantly, under this condition the acetyl-CoA generated by β-oxidation will tend to deplete inhibitory oxaloacetate through the action of citrate synthase, making site II_F more prone to generate superoxide/H_2O_2 [18].

With palmitoylcarnitine plus carnitine as substrate, the total observed rate of H_2O_2 production was 199 pmol H_2O_2 min^{-1} mg $protein^{-1}$. From the redox states of the reporters and the corrected effects of malonate on H_2O_2 production, we were able to account for the entirety of this observed H_2O_2 production. There were approximately equal contributions from sites II_F (38%) and III_{Qo} (36%), with site I_F producing slightly less (25%) (Fig. 5). The absence of unaccounted-for H_2O_2 production indicated that neither site I_Q nor the ETF/ETF:QOR system generated substantial superoxide/H_2O_2. Indeed, the ETF/ETF:QOR system does not generate measureable superoxide/H_2O_2 except under very specific conditions and in the presence of respiratory chain inhibitors [18].

Sites of superoxide/H_2O_2 production during oxidation of glutamate plus malate

In the final condition, the substrate pair glutamate plus malate was used to generate NADH (Fig. 3d). During oxidation of this substrate combination, malate is oxidized to oxaloacetate by malate dehydrogenase and NADH is generated. Glutamate is used to transaminate the oxaloacetate to form aspartate and 2-oxoglutarate (and some glutamate may be oxidized to 2-oxoglutarate by glutamate dehydrogenase). The aspartate is exchanged for glutamate on the glutamate–aspartate antiporter, and much of the 2-oxoglutarate is exchanged for malate on the oxoglutarate–malate antiporter (although some may be oxidized by 2-oxoglutarate dehydrogenase). In this way, removal of oxaloacetate maximizes NADH generation by malate dehydrogenase [31].

With glutamate plus malate as substrate, the total observed rate of H_2O_2 production was 182 pmol H_2O_2 min^{-1} mg $protein^{-1}$. Under this condition, sites I_F and III_{Qo} contributed equally (30% each) [21] (Fig. 5). Malonate did not significantly inhibit the rate (3% inhibition ± 5%), so site II_F was not a significant contributor, presumably because it was inhibited by oxaloacetate or malate under these conditions [15]. A significant proportion (41%) of the total H_2O_2 production was unassigned, indicating that another site also contributed under this condition. We assume this was from forward flow through OGDH (Fig. 5) because some 2-oxoglutarate was likely formed during transamination of glutamate, but we cannot exclude a contribution from site I_Q or uncharacterized other sites in this complex metabolic condition. In principle the contribution of site I_Q could be assessed by the decrease in rate observed following addition of rotenone after correction for secondary changes in other defined sites, but definitive conclusions could not be drawn because of the relatively small rates of unassigned H_2O_2 production, large changes in redox states of the reporters following addition of rotenone, relatively large errors involved, and possible changes in other uncharacterized sites following addition of rotenone.

Advantages and limitations of the approach used

The great strength of the approach we have used here to measure the contributions of different sites to overall mitochondrial H_2O_2 production [21] is that, unlike all previous approaches, it reports rates under native conditions in the absence of added inhibitors. This gives it great potential for future studies with physiological substrate mixes in mitochondria and in intact cells and organisms. Its main limitation is the assumption that the calibration curves measured in the presence of inhibitors and particular substrates apply under native conditions using other substrates. The good agreement between calculated and measured total rates (Fig. 5) supports the validity of this assumption.

Potential pathological and physiological implications

The results obtained using the four different substrates described in Fig. 5 provide a very clear illustration of the remarkably different H_2O_2-producing profiles that can be attained by isolated muscle mitochondria oxidizing conventional substrates. When taken as a whole, two results are striking. (i) The native rates differed greatly between substrates. This implies that mitochondrial superoxide/H_2O_2 production rates *in vivo* likely depend critically on the substrate being oxidized, so physiological or pathological changes in substrate may be very important determinants of rates of radical production, even at the same overall rate of oxygen consumption. (ii) The contribution of each site differed markedly between substrates. With succinate, site I_Q dominated, with relatively small contributions from sites I_F and III_{Qo}. However, with palmitoylcarnitine plus carnitine, site II_F was an important contributor, and with glycerol 3-phosphate, five sites contributed, including site II_F and mGPDH. Thus, which sites contribute to superoxide and H_2O_2 production in mitochondria, in cells, and *in vivo* under both physiological and pathological conditions likely depends critically on the substrates being utilized.

Notably, the sites are known to differ markedly in the topology of superoxide production [6,16,27,32,33]. Essentially all superoxide/H_2O_2 from sites I_F, I_Q and II_F is directed to the matrix, but about half the superoxide from site III_{Qo} and mGPDH appears in the intermembrane space. Thus, the strength of mitochondrial superoxide signaling in the cytosol (and also the amount of oxidative damage caused by superoxide and H_2O_2 in the matrix) will differ substantially between substrates, even at identical total rates of mitochondrial superoxide/H_2O_2 production.

Acknowledgments

Supported by National Institutes of Health grants P01 AG025901, PL1 AG032118, R01 AG03354 and TL1 AG032116 (M.D.B., C.L.Q.) and The Ellison Medical Foundation, grant AG-SS-2288-09 (M.D.B., I.V.P.). Fellowship support was from The Glenn Foundation (I.V.P) and The Carlsberg Foundation (M.H-M).

References

[1] S.K. Powers, J. Duarte, A.N. Kavazis, E.E. Talbert, Reactive oxygen species are signalling molecules for skeletal muscle adaptation, Experimental Physiology 95 (2010) 1–9.
[2] S.J. Ralph, J. Neuzil, Mitochondria as targets for cancer therapy, Molecular Nutrition and Food Research 53 (2009) 9–28.
[3] M. Sundaresan, Z.X. Yu, V.J. Ferrans, K. Irani, T. Finkel, Requirement for generation of H_2O_2 for platelet-derived growth factor signal transduction, Science 270 (1995) 296–299.
[4] M.E. Witte, J.J. Geurts, H.E. de Vries, P. van der Valk, J. van Horssen, Mitochondrial dysfunction: a potential link between neuroinflammation and neurodegeneration? Mitochondrion 10 (2010) 411–418.
[5] M.P. Murphy, How mitochondria produce reactive oxygen species, Biochemical Journal 417 (2009) 1–13.
[6] M.D. Brand, The sites and topology of mitochondrial superoxide production, Experimental Gerontology 45 (2010) 466–472.
[7] A. Boveris, N. Oshino, B. Chance, The cellular production of hydrogen peroxide, Biochemical Journal 128 (1972) 617–630.
[8] J.R. Treberg, C.L. Quinlan, M.D. Brand, Evidence for two sites of superoxide production by mitochondrial NADH-ubiquinone oxidoreductase (complex I), Journal of Biological Chemistry 286 (2011) 27103–27110.
[9] D.M. Kramer, A.G. Roberts, F. Muller, J.L. Cape, M.K. Bowman, Q-cycle bypass reactions at the Q_o site of the cytochrome bc_1 (and related) complexes, Methods in Enzymology 382 (2004) 21–45.

[10] F.L. Muller, A.G. Roberts, M.K. Bowman, D.M. Kramer, Architecture of the Q_o site of the cytochrome bc_1 complex probed by superoxide production, Biochemistry 42 (2003) 6493–6499.
[11] C.L. Quinlan, A.A. Gerencser, J.R. Treberg, M.D. Brand, The mechanism of superoxide production by the antimycin-inhibited mitochondrial Q-cycle, Journal of Biological Chemistry 286 (2011) 31361–31372.
[12] V.I. Bunik, C. Sievers, Inactivation of the 2-oxo acid dehydrogenase complexes upon generation of intrinsic radical species, European Journal of Biochemistry 269 (2002) 5004–5015.
[13] L. Tretter, V. Adam-Vizi, Generation of reactive oxygen species in the reaction catalyzed by alpha-ketoglutarate dehydrogenase, Journal of Neuroscience 24 (2004) 7771–7778.
[14] A.A. Starkov, G. Fiskum, C. Chinopoulos, B.J. Lorenzo, S.E. Browne, M.S. Patel, M.F. Beal, Mitochondrial alpha-ketoglutarate dehydrogenase complex generates reactive oxygen species, Journal of Neuroscience 24 (2004) 7779–7788.
[15] C.L. Quinlan, A.L. Orr, I.V. Perevoshchikova, J.R. Treberg, B.A. Ackrell, M.D. Brand, Mitochondrial complex II can generate reactive oxygen species at high rates in both the forward and reverse reactions, Journal of Biological Chemistry 287 (2012) 27255–27264.
[16] A.L. Orr, C.L. Quinlan, I.V. Perevoshchikova, M.D. Brand, A refined analysis of superoxide production by mitochondrial sn-glycerol 3-phosphate dehydrogenase, Journal of Biological Chemistry 287 (2012) 42921–42935.
[17] E.L. Seifert, C. Estey, J.Y. Xuan, M.E. Harper, Electron transport chain-dependent and -independent mechanisms of mitochondrial H_2O_2 Emission during long-chain fatty acid oxidation, Journal of Biological Chemistry 285 (2010) 5748–5758.
[18] I.V. Perevoshchikova, C.L. Quinlan, A.L. Orr, M.D., Brand. Sites of superoxide and hydrogen peroxide production during fatty acid oxidation in rat skeletal muscle. Free Radical Biology and Medicine 61, 2013, 298–309.
[19] T.A. White, N. Krishnan, D.F. Becker, J.J. Tanner, Structure and kinetics of monofunctional proline dehydrogenase from *Thermus thermophilus*, Journal of Biological Chemistry 282 (2007) 14316–14327.
[20] J.H. Forman, J. Kennedy, Superoxide production and electron transport in mitochondrial oxidation of dihydroorotic acid, Journal of Biological Chemistry 250 (1975) 4322–4326.
[21] C.L. Quinlan, J.R. Treberg, I.V. Perevoshchikova, A.L. Orr, M.D. Brand, Native rates of superoxide production from multiple sites in isolated mitochondria measured using endogenous reporters, Free Radical Biology and Medicine 53 (2012) 1807–1817.
[22] C. Affourtit, C.L. Quinlan, M.D. Brand, Measurement of proton leak and electron leak in isolated mitochondria, Methods in Molecular Biology 810 (2012) 165–182.
[23] J.R. Treberg, C.L. Quinlan, M.D. Brand, Hydrogen peroxide efflux from muscle mitochondria underestimates matrix superoxide production—a correction using glutathione depletion, FEBS Journal 277 (2010) 2766–2778.
[24] R.G. Hansford, B.A. Hogue, V. Mildaziene, Dependence of H_2O_2 formation by rat heart mitochondria on substrate availability and donor age, Journal of Bioenergetics and Biomembrane 29 (1997) 89–95.
[25] A.J. Lambert, M.D. Brand, Superoxide production by NADH:ubiquinone oxidoreductase (complex I) depends on the pH gradient across the mitochondrial inner membrane, Biochemical Journal 382 (2004) 511–517.
[26] L. Kussmaul, J. Hirst, The mechanism of superoxide production by NADH: ubiquinone oxidoreductase (complex I) from bovine heart mitochondria, Proceedings of the National Academy of Sciences of the USA 103 (2006) 7607–7612.
[27] J. St-Pierre, J.A. Buckingham, S.J. Roebuck, M.D. Brand, Topology of superoxide production from different sites in the mitochondrial electron transport chain, Journal of Biological Chemistry 277 (2002) 44784–44790.
[28] F.L. Muller, Y. Liu, M.A. Abdul-Ghani, M.S. Lustgarten, A. Bhattacharya, Y.C. Jang, H. Van Remmen, High rates of superoxide production in skeletal-muscle mitochondria respiring on both complex I- and complex II-linked substrates, Biochemical Journal 409 (2008) 491–499.
[29] F. Zoccarato, L. Cavallini, A. Alexandre, Succinate is the controller of O_2^-/H_2O_2 release at mitochondrial complex I: negative modulation by malate, positive by cyanide, Journal of Bioenergetics and Biomembranes 41 (2009) 387–393.
[30] F. Zoccarato, L. Cavallini, S. Bortolami, A. Alexandre, Succinate modulation of H_2O_2 release at NADH:ubiquinone oxidoreductase (Complex I) in brain mitochondria, Biochemical Journal 406 (2007) 125–129.
[31] D.G. Nicholls, S.J. Ferguson, Bioenergetics 3, Academic Press, London , 2002.
[32] S. Miwa, M.D. Brand, The topology of superoxide production by complex III and glycerol 3-phosphate dehydrogenase in Drosophila mitochondria, Biochimica Biophysica Acta 1709 (2005) 214–219.
[33] F.L. Muller, Y. Liu, H. Van Remmen, Complex III releases superoxide to both sides of the inner mitochondrial membrane, Journal of Biological Chemistry 279 (2004) 49064–49073.